Promiscuous and selective: how intrinsically disordered BH3-proteins interact with their pro-survival partner MCL-1.

Liza Dahal, Tristan O.C. Kwan, Jeffery J. Hollins and Jane Clarke[1]

[1]Corresponding author, Email: jc162@cam.ac.uk

Department of Chemistry, University of Cambridge, Lensfield Road, Cambridge, CB2 1EW

Highlights

- Despite differences in residual helicity BH3 peptides bind equally fast to MCL-1.
- Differences in stabilities results from off-rates, altering complex lifetimes.
- This difference arises from variation in interactions at MCL-1 binding interface.

GRAPHICAL ABSTRACT

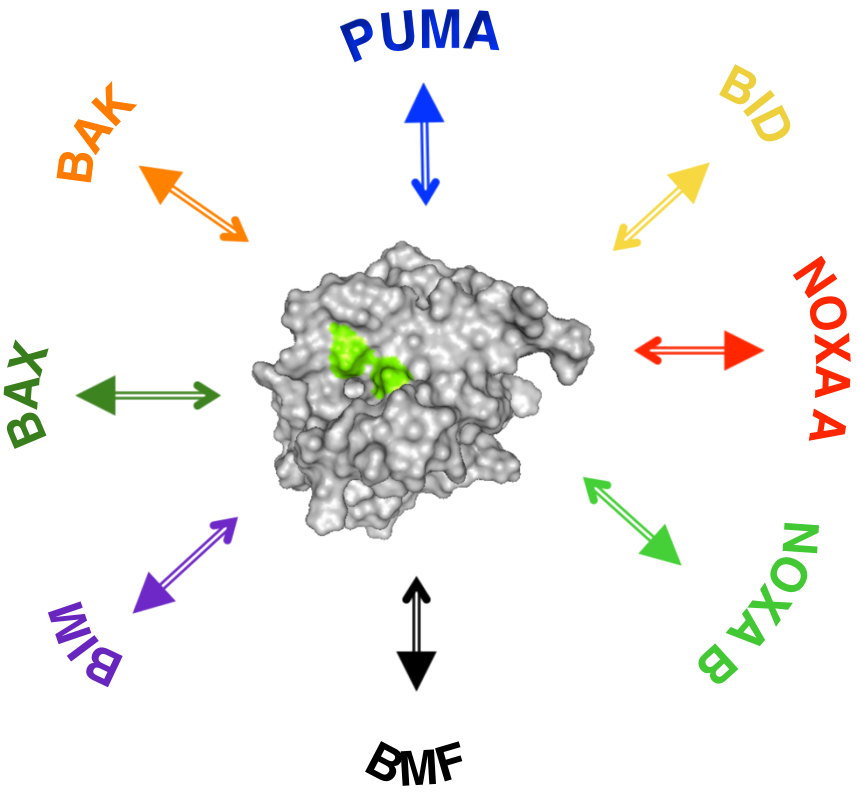

Promiscuous and selective: how intrinsically disordered BH3-proteins interact with their pro-survival partner MCL-1.

Liza Dahal, Tristan O.C. Kwan, Jeffery J. Hollins and Jane Clarke[1]

[1]Corresponding author, Email: jc162@cam.ac.uk

Department of Chemistry, University of Cambridge, Lensfield Road, Cambridge, CB2 1EW

Abstract [1]

The BCL-2 family of proteins plays a central role in regulating cell survival and apoptosis. Disordered BH3-only proteins bind promiscuously to a number of different BCL-2 proteins, with binding affinities that vary by orders of magnitude. Here we investigate the basis for these differences in affinity. We show that eight different disordered BH3 proteins all bind to their BCL-2 partner (MCL-1) very rapidly, and that the differences in sequences result in different dissociation rates. Similarly, mutation of the binding surface of MCL-1 generally affects association kinetics in the same way for all BH3 peptides but has significantly different effects on the dissociation rates. Importantly, we infer that evolution of homologous, competing complexes has resulted in producing complexes with significantly different lifetimes.

[1] BCL-2 : B cell lymphoma-2

MCL-1 : Myeloid cell leukemia 1

A1: BCL-2-related gene A1

BAK: BCL-2 antagonist killer 1

BAX: BCL-2 associated X protein

CD: Circular Dichroism

wt: wild-type

Introduction

The physiological process of cell death, or apoptosis, is a highly regulated process and the B cell lymphoma-2 (BCL-2) family of proteins are important molecular arbitrators of the process[1, 2]. To date, five anti-apoptotic (BCL-2, BCL-xl, BCL-w, Myeloid cell leukemia 1 (MCL-1) and BCL-2-related gene A1 (A1)) and at least two pro-apoptotic BCL-2 proteins (BCL-2 antagonist killer 1 (BAK) and BCL-2-associated X protein (BAX)) have been identified[3, 4]. A third group of ten pro-apoptotic proteins (termed BCL-2 homology domain (BH3)-only) are thought to interact with both pro-apoptotic BAK and BAX and also the anti-apoptotic proteins[5-7]. The BH3-only proteins can be divided into two groups; Activators (BIM, BID and PUMA) and Sensitizers (NOXA A, NOXA B, BMF, BIK, BAD, HRK)[8]. Several models have been proposed to understand the role of these pro and anti-apoptotic BCL-2 proteins[8]. In all these models, differences in affinity between the anti-apoptotic proteins and the pro-apoptotic proteins are predicted to determine their mode of action. These BCL-2 family proteins have a homologous BH3 domain, which is intrinsically disordered in isolation, but form a contiguous helical segment upon binding to its partner BCL-2 proteins[9-13]. This disordered nature is likely be the source of promiscuity as well as selective binding, thus increasing the diversity and flexibility of this intricate network.

The sequence alignment of eight BH3 peptides calculated using Clustal Omega[14, 15], shows that there are only two absolutely conserved residues, although they all fold to the same structure upon binding - the calculated RMSD values show that the complexes of PUMA, NOXA A, NOXA B, BIM, BID and BAX with MCL-1 have high structural homology (Fig.1 A and C). Previous studies have shown that BH3 peptides bind to anti-apoptotic MCL-1 with different affinities[2, 16, 17].

Here, we compare the interaction of eight BH3 peptides with MCL-1, by using kinetic and thermodynamic analyses to understand the biophysical nature of these interactions. Our results show that the association rates are within the same order of magnitude but there are large differences in the dissociation rates. We further investigate two mutants of MCL-1 that have previously been shown to increase the association rate constant of the PUMA peptide and find similar results for all the BH3 peptides investigated in this study[18]. Our results are in line with our previous hypothesis that the BH3 binding groove of MCL-1 opens up to allow binding of the BH3 peptides[18]. Interestingly, we see larger differences in dissociation rate constants but the effect on off-rates is different for different peptides. Hence, the affinity of BH3 peptides to MCL-1 is controlled by dissociation rate, which is a result of differences in the specific interactions of the BH3 peptides at the MCL-1 binding interface. The results presented here provide insight into the underlying molecular basis for both the promiscuity and the selectivity afforded by these structurally homologous complexes of BH3 peptides with pro-survival MCL-1.

Results

Different sequences impart different degrees of disorder

Circular dichroism (CD) spectra reveal that the BH3 peptides investigated are mainly disordered under our experimental conditions. However, the percentage helicities of the BH3 peptides calculated from MRE value at 222 nm[19], ranges between approximately 9-63% (Fig 1B). Percentage helicity for the BH3 peptides estimated from CD does not correlate with predicted percentage helicity from Agadir[20-22], or the predicted percentage disorder from PONDR VSL2[23-30], ESpritz (X-Ray)[31-35] and ANCHOR[36, 37](Fig S1).

Differences in affinity is due to differences in k_{off}

We investigated the kinetic signatures of seven different peptides (BID, BIM, BMF, NOXA A, NOXA B, BAK, BAX) and compared it with previously published data for PUMA [18] interacting with wild-type (wt) MCL-1 (Table 1). The association rate constants, k_{on}, vary by only an order of magnitude for all the peptides investigated (Fig. 2A, Fig. 3A). On the other hand, the dissociation rate constants, k_{off}, differ by approximately four orders of magnitude (Fig. 2B, Fig. 3B). The equilibrium dissociation constants, K_d, also differ by four-five orders of magnitude and reflect the pattern of k_{off} (Fig. 3C).

Kinetic effects of mutation of MCL-1 binding interface

To investigate the role of partner protein in the interaction we studied two MCL-1 mutations (V234A and T247A) in the binding groove (Table 2). We had previously shown that these mutations, although they weaken binding, actually slightly increase the association rate constant (k_{on}) of wild-type PUMA[18]. Similarly, all BH3 peptides (except BAX) in our experiments have somewhat enhanced association rates to the MCL-1 mutants, with k_{on} increased by up to 4-fold, compared to wt (Fig. 4, Fig. S2). However, the effect of mutation in the binding groove of MCL-1 on dissociation rates differs by up to ~40-fold for different BH3 peptides, with some seeing a faster and some slower off-rates compared to wt MCL-1 (Fig.4).

Discussion

The K_d values calculated from the kinetics data are presented in Tables 1 and 2. The activator BH3 peptides (PUMA BID and BIM) all have sub-nM affinities. The sensitizers are known to display more specificity in their binding, so NOXA B, known to bind MCL-1 specifically also has sub-nM affinity whereas NOXA A and, in particular, BMF, bind more weakly. As expected, the effector, pro-apoptotic peptides BAK and BAX bind less tightly than the activator proteins (Table 1). These data are more-or-less consistent with

previously reported affinities for BH3 proteins interacting with wt MCL-1; given the differences in experimental conditions [2, 16, 17].

Due to the abundance of charged residues and their disordered nature, IDPs are susceptible to changes in ionic strength and solvent environments[38, 39]. Patterning of charges is also known to affect the overall conformational ensembles of IDPs[27, 40, 41]. As increased residual structure in free IDP has been seen to increase affinity of IDPs to partner proteins, we investigated whether there is a relationship between residual helicity of the peptides and our kinetic and thermodynamic data[42, 43]. As shown in Supplementary Fig. S3, although differences in sequence result in differences in residual helicity of the BH3 peptides, we see no correlation between residual helicity and k_{on}, k_{off} or K_d (Fig.S3).

k_{on} values observed for all the BH3 peptides are within the range of association kinetics reported for most IDP:protein interactions (~10^5 - 10^8 $M^{-1}s^{-1}$)[44, 45]. However, despite differences in sequences, all the BH3-only peptides bind to wt MCL-1 with a similar association rate (Note that the scale in Fig 3A is very different to that of Figs. 3B or 3C). Since, the BH3 peptides have only 6% sequence identity, the estimated charges of the peptides are varied, and we see that the k_{on} is related to the estimated charge on the peptide (Fig. S4). Note that our experiments were conducted in a buffer of ionic strength = 100mM. Previous studies of the PUMA : MCL-1 interaction (PUMA has an estimated charge of ~-3 in our experimental conditions) have shown that increasing ionic strength slows the association of PUMA[46]. The fold-change from an ionic strength of 0 to infinite ionic strength is some 20-fold (although this is also ion-type dependent)[47]. However, variations in the physiological range (100-200 mM) affect the association rate by only approximately 2-fold[47]. Thus, these marginal differences in k_{on} observed for the BH3 peptides binding to MCL-1 may simply be due largely to differences in the charges

of the peptides, as was seen for a similar comparative study of different IDP ligands binding to KIX[48].

However, we find that the dissociation rate constants (k_{off}) of the BH3 peptides from MCL-1 differ by 4-orders of magnitude. The results clearly reveal that differences in affinity reflect differences in the rate at which BH3 peptides dissociate (Fig. 5). This behavior has been observed for other IDP systems where the effect of post-translational modification (phosphorylation in pKID/KIX) and conserved helix flanking prolines (conserved prolines in MLL/KIX and p53/MDM2) were investigated[49, 50]. The results from these papers and the results presented here, suggest that different characteristic of IDPs primarily allow modulation of lifetimes of the IDP/partner complexes. This behavior of stability in signaling proteins being controlled by dissociation rate has been previously proposed to be functionally relevant[50-52]. Perhaps being disordered allows IDPs involved in complex network and signaling pathways, such as BH3 proteins, to adapt their kinetics allowing them to bind/unbind to many target proteins with different kinetics; that is, allowing promiscuous binding. This may also be why disorder is conserved and abundant in proteins involved in cell signaling processes[53-55].

A structural alignment of the available complex structures of BH3 peptides (PUMA, BID, BIM, NOXA A, NOXA B and BAX) with MCL-1 (Fig 1C) reveals a close structural homology of these complex structures, with RMSDs 1.2 - 3.5 Å (Fig 1C). All BH3 peptides bind to the same 'BH3-binding' groove in MCL-1 and only minor structural differences are observed in the structural alignment. Analysis of the contacts formed, however, show that each peptide binds MCL-1 using a different subset of binding residues, similar to that suggested for A1[56] (Fig. S5). Previous NMR chemical shift analysis indicated similar changes in MCL-1 conformation upon BH3 peptide binding, suggesting that MCL-1 accommodates each BH3 ligand in a similar manner[11, 57]. Our results for the two conservative MCL-1 interface mutants (V234A and T247A), show that

although the effect on association kinetics is the same for all the BH3 peptides (i.e. we see marginal increase in association rates compared to wt MCL-1), the effects on the affinity of the complex (and thus the off-rates) is very different. Mutating the residues of MCL-1 causes changes in affinity by affecting the dissociation rate constant. In some cases, the effect is marginal, but in others the affinity changes by orders of magnitude. Furthermore, while most complexes are destabilized by mutation of interface residues in MCL-1, in others affinity is increased by several orders of magnitude (Fig 4). Interestingly, although the loss in affinity ($\Delta\Delta G$) is correlated with the number of contacting residues in the peptide for the MCL-1 mutant V234A, there is no such correlation for the T247A mutant (Fig. S5, Table 2). We infer that there may be small adjustments of the structure of the peptide when binding to a mutant MCL-1. Thus, the differences in affinity are regulated by differences in specific contacts with the BCL-2-like partner (in our case MCL-1).

Concluding Remarks

We find that varying the dissociation rates essentially controls the affinity of a BCL-2 protein, MCL-1, with different BH3 peptides. These differences in affinity are largely due to different interactions formed at the MCL-1 binding interface once the complex structure matures. Evolution of these homologous and competing complexes has resulted in different stabilities by modulation of the off-rates of these complexes. We infer that it is the lifetime of the complex that may be the most important biophysical property in a competing network, such as the BH3:BCL-2 system.

Material and Methods

Biophysical buffer

All biophysical experiments were carried out in 50mM sodium phosphate buffer (0.05% Tween20), pH 7.0.

Protein expression and purification

Wild-type MCL-1 and mutants thereof (*Mus musculus*, 152-308 residues, Uniprot P97287) were expressed as described previously.[46] The harvested cells after expression were resuspended in 1*PBS 25mM Imidazole, pH 7.5 and sonicated. The sonicate was centrifuged and the supernatant incubated with Ni^{2+}- agarose resin for 1 hour at 4ºC. The protein bound to the Ni^{2+}- agarose resin was then eluted with 1*PBS 500mM Imidazole (pH 7.5-8) and 2mM ethylenediaminetetraacetic acid (EDTA) was added to the elution to prevent precipitation. The protein solution was then buffer exchanged to 1*PBS 25mM Imidazole, pH 7.5 using a 5kDa molecular weight cut off spin column. 600 units of thrombin was then added to the protein solution and left overnight at room temperature to cleave off the HisTag. Thrombin cleaved supernatant supplemented with 2mM $CaCl_2$ to sequester the EDTA, was incubated with Ni^{2+}- agarose resin for 1 hour to remove uncleaved protein. Cleaved protein was loaded into 5mL HiTrap™ SP HP ion-exchange pre-equilibrated with 10mM HEPES, pH 7.5, and eluted using 1M NaCl buffer gradient. The protein was then loaded into Superdex G75 gel filtration column to elute with the biophysical buffer, 50mM Sodium phosphate (0.05% Tween20) pH7.0. Eluted protein was confirmed to be MCL-1 after analysis by gel electrophoresis and mass spectroscopy and stored at 4ºC.

PUMA peptide with 35 residues (*Mus musculus*, 127-161 residues, Uniprot Q99ML1) with M144A mutation was expressed as described previously.[58] The purification was also carried out as described before except that after binding to the Ni^{2+} agarose resin,

the resin was washed with 20mM Tris pH7.0, 10 mM imidiazole buffer and cleaved with Factor Xa in 20mM Tris, 50mM NaCl, 5mM $CaCl_2$, pH 8.0 buffer. The cleaved supernatant was then purified by ion-exchange using 10mM Tris, pH8 and a linear gradient of 1M NaCl was applied and the protein eluted at 12-17%. The peptide was then further purified using Superdex G30 gel filtration column and eluted with the biophysical buffer, 50mM Sodium phosphate (0.05% Tween20) pH7.0. PUMA peptides were then frozen using liquid N2, and stored at -80ºC.

Peptides

All BH3 peptides (Uniprot code: PUMA - Q99ML1, BID - P70444, BIM - O54918, BMF – Q91ZE9, NOXA A – Q9JM54, NOXA B – Q9JM54, BAK – Q16611, and BAX – Q07812; 35 amino acids, labeled with TAMRA dye at the N-terminus) were purchased from Biomatik. Peptides were dissolved in the biophysical buffer as required and filtered using a 0.22 mm cutoff filter. The stock solutions of peptides were frozen using liquid N_2 and stored at -80ºC.

Estimated parameters for peptides and PDB complex structures

Estimated peptide charges were calculated using pK_a values of amino acids for model peptides[59] and corrected for addition of TAMRA dye at the N-terminus. Agadir % helicity predictions were made for pH 7.0, 25 ºC and 100mM ionic strength[20-22]. Percentage (%) disorder predictions were generated using the tools PONDR-VSL2[23-25, 28-30], ESpritz (X-Ray - chosen as the peptides are only 35 residues long and most have X-ray structures of bound complex with their partners available in the PDB)[31-35] and ANCHOR[36, 37]. To create the contact map, contacting residues of BH3 peptides PUMA, NOXA A, NOXA B, BIM, BID and BAX with MCL-1 were plotted from PDB structures 2ROC, 2ROC, 2JM6, 2PQK, 2KBW and 3PK1. Contacts between the peptides and MCL-1 were defined between all non-hydrogen atoms within 4Å. Structural alignment for PDB structures

(2ROC, 2ROD, 2JM6, 2PQK, 2KBW and 3PK1) were built using PyMOL and RMSD values reported for each.

Concentration measurements

The concentrations of purified protein, MCL-1 (wild-type and mutants) and PUMA peptide were measured by absorbance at 280nm and calculated using extinction coefficients 22157 $M^{-1}cm^{-1}$ [46] and 7113 $M^{-1}cm^{-1}$ [18] respectively. The extinction coefficients were previously determined using amino acid analysis.

TAMRA labeled peptide concentrations were determined from absorbance at 555nm, using extinction coefficient 83000 $M^{-1}cm^{-1}$. The extinction coefficient was again calculated by amino acid analysis of multiple peptide samples.

Circular Dichorism (CD) and residual helicity

Samples were prepared at different concentrations using the biophysical buffer. CD spectra (190-260 nm) were recorded in a 2mm path-length cuvette at 25ºC using a ChiraScan CD spectrometer from Applied Photophysics. All spectra were buffer subtracted and estimate for percentage helicities were calculated using average mean ellipticity at 222nm using the methods described previously[19].

Kinetic measurements

For all kinetic experiments, an excitation wavelength of 555nm was used and emission above 570nm was measured.

Association kinetics experiments were performed using a SX18 or SX20 fluorescence stopped-flow spectrometer from Applied Photophysics with the temperature maintained at 25ºC. Experiments were performed with 10-fold or larger excess of the folded partner (wild-type and mutant MCL-1) over TAMRA labeled BH3 peptides. An average of 30-40 traces were fitted to an equation describing a single exponential process to extract the observed rate (k_{obs}) for each concentration of the partner protein. The dependence of

k_{obs} on the concentration of the partner protein was fit to a straight line, and the gradient of the line used to determine the association rate constant (k_{on}). Fluorescence polarization accessory was used to measure anisotropy change instead of fluorescence change where signal change was poor.

Out-competition dissociation kinetics experiments at 25ºC were carried out using SX18 and SX20 fluorescence stopped-flow spectrometer from Applied Photophysics for k_{obs} > $0.03s^{-1}$ or a Varian Cary Eclipse spectrophotometer for k_{obs} < 0.03 s^{-1}. A pre-formed complex of the partner protein and the TAMRA labeled BH3 peptides was mixed with different concentrations of unlabeled PUMA peptide, used as a competitor in these experiments. A change in fluorescence upon dissociation of the TAMRA labeled peptides was monitored and fitted to a single exponential equation to determine the k_{obs}. In some cases, the change in fluorescence signal upon dissociation of the TAMRA labeled peptides was very small to monitor, therefore a fluorescence polarization accessory was used to monitor the change in anisotropy instead. As a large excess of the competitor was used the k_{obs} represents the dissociation rate (k_{off}).

Acknowledgements

The authors would like to thank Dr Joseph M. Rogers for use of data describing PUMA interacting with wild-type and mutants of MCL-1. We would also like to thank Dr Sarah L. Shammas for helpful discussions.

This work was supported by the Wellcome Trust (grant number WT095195). J.C. is a Wellcome Trust Senior Research Fellow. L.D. is supported by an Engineering and Physical Sciences Research Council (UK) studentship.

References

1. Huang D. C., Strasser A. (2000). BH3-only proteins-essential initiators of apoptotic cell death. Cell. 103, 839-842.
2. Chen L., Willis S. N., Wei A., Smith B. J., Fletcher J. I., Hinds M. G., et al. (2005). Differential targeting of prosurvival Bcl-2 proteins by their BH3-only ligands allows complementary apoptotic function. Mol. Cell. 17, 393-403.
3. Moldoveanu T., Follis A. V., Kriwacki R. W., Green D. R. (2014). Many players in BCL-2 family affairs. Trends Biochem. Sci. 39, 101-111.
4. Zheng J. H., Follis A. V., Kriwacki R. W., Moldoveanu T. (2016). Discoveries and controversies in BCL-2 protein-mediated apoptosis. FEBS J. 283, 2690-2700.
5. Kale J., Liu Q., Leber B., Andrews D. W. (2012). Shedding light on apoptosis at subcellular membranes. Cell. 151, 1179-1184.
6. Hinds M. G., Smits C., Fredericks-Short R., Risk J. M., Bailey M., Huang D. C. S., et al. (2007). Bim, Bad and Bmf: intrinsically unstructured BH3-only proteins that undergo a localized conformational change upon binding to prosurvival Bcl-2 targets. Cell Death Differ. 14, 128-136.
7. Vela L., Gonzalo O., Naval J., Marzo I. (2013). Direct interaction of bax and bak proteins with Bcl-2 homology domain 3 (BH3)-only proteins in living cells revealed by fluorescence complementation. J. Biol. Chem. 288, 4935-4946.
8. Shamas-Din A., Brahmbhatt H., Leber B., Andrews D. W. (2011). BH3-only proteins: Orchestrators of apoptosis. Biochim. Biophys. Acta, Mol. Cell Res. 1813, 508-520.
9. Hinds M. G., Day C. L. (2005). Regulation of apoptosis: Uncovering the binding determinants. Curr. Opin. Struct. Biol. 15, 690-699.
10. Liu X., Dai S., Zhu Y., Marrack P., Kappler J. W. (2003). The structure of a Bcl-xL/Bim fragment complex: Implications for Bim function. Immunity. 19, 341-352.
11. Day C. L., Smits C., Fan F. C., Lee E. F., Fairlie W. D., Hinds M. G. (2008). Structure of the BH3 domains from the p53-inducible BH3-only proteins Noxa and Puma in complex with Mcl-1. J. Mol. Biol. 380, 958-971.
12. Sattler M., Liang H., Nettesheim D., Meadows R. P., Harlan J. E., Eberstadt M., et al. (2009). Structure of Bcl-xL-Bak peptide complex : Recognition between regulators of apoptosis. Science. 983, 983-987.
13. Rautureau G. J. P., Day C. L., Hinds M. G. (2010). Intrinsically disordered proteins in Bcl-2 regulated apoptosis. Int. J. Mol. Sci. 11, 1808-1824.
14. Goujon M., McWilliam H., Li W., Valentin F., Squizzato S., Paern J., et al. (2010). A new bioinformatics analysis tools framework at EMBL-EBI. Nucleic Acids Res. 38, 695-699.
15. Sievers F., Wilm A., Dineen D., Gibson T. J., Karplus K., Li W., et al. (2011). Fast, scalable generation of high-quality protein multiple sequence alignments using Clustal Omega. Mol. Syst. Biol. 7.
16. Ku B., Liang C., Jung J. U., Oh B. H. (2011). Evidence that inhibition of BAX activation by BCL-2 involves its tight and preferential interaction with the BH3 domain of BAX. Cell Res. 21, 627-641.

17. Kvansakul M., Hinds M. G. (2013). Structural biology of the Bcl-2 family and its mimicry by viral proteins. Cell Death Dis. 4, e909-910.
18. Rogers J. M., Oleinikovas V., Shammas S. L., Wong C. T., De Sancho D., Baker C. M., et al. (2014). Interplay between partner and ligand facilitates the folding and binding of an intrinsically disordered protein. Proc. Natl. Acad. Sci. U.S.A. 111, 15420-15425.
19. Muñoz V., Serrano L. (1995). Elucidating the folding problem of helical peptides using empirical parameters. II. Helix macrodipole effects and rational modification of the helical content of natural peptides. J. Mol. Biol. 245, 275-296.
20. Munoz V., Serrano L. (1994). Elucidating the folding problem of helical peptides using empirical parameters. Nat. Struct. Biol. 1, 399-409.
21. Munoz V., Serrano L. (1997). Development of the multiple sequence approximation within the AGADIR model of a-Helix formation: Comparison with Zimm–Bragg and Lifson–Roig Formalisms. Biopolymers. 41, 495-509.
22. Lacroix E., Viguera A. R., Serrano L. (1998). Elucidating the folding problem of alpha-helices: local motifs, long- range electrostatics, ionic-strength dependence and prediction of NMR parameters. J. Mol. Biol. 284, 173-191.
23. Garner E., Romero P., Dunker A. K., Brown C. J., Obradovic Z. (1999). Predicting binding regions within disordered proteins. Genome Inf. Ser. 10, 41-50.
24. Li X., Romero P., Rani M., Dunker A. K., Obradovic Z. (1999). Prediction protein disorder for N-, C-, and internal regions. Genome Inf. Ser. 10, 30-40.
25. Romero P., Obradovic Z., Dunker A. K. (1997). Sequence data analysis for long disordered regions prediction in the calcineurin family. Genome Inf. Ser. 8, 110-124.
26. Uversky V. N., Gillespie J. R., Fink A. L. (2000). Why are 'natively unfolded' proteins unstructured under physiologic conditions? Proteins: Struct., Funct., Genet. 41, 415-427.
27. Romero P., Obradovic Z., Li X., Garner E. C., Brown C. J., Dunker A. K. (2001). Sequence complexity of disordered protein. Proteins: Struct., Funct., Genet. 42, 38-48.
28. Vucetic S., Brown C. J., Dunker A. K., Obradovic Z. (2003). Flavors of protein disorder. Proteins: Struct., Funct., Genet. 52, 573-584.
29. Radivojac P., Obradović Z., Brown C. J., Dunker A. K. (2003). Prediction of boundaries between intrinsically ordered and disordered protein regions. Pac. Symp. Biocomput. 227, 216-227.
30. Obradovic Z., Peng K., Vucetic S., Radivojac P., Brown C. J., Dunker A. K. (2003). Predicting intrinsic disorder from amino acid sequence. Proteins: Struct., Funct., Genet. 53, 566-572.
31. Pollastri G., Przybylski D., Rost B., Baldi P. (2002). Improving the prediction of protein secondary structure in three and eight classes using recurrent neural networks and profiles. Proteins: Struct., Funct., Genet. 47, 228-235.
32. Sperduti A., Starita A. (1997). Supervised neural networks for the classification of structures. Neural Networks, IEEE Transactions on 8, 714-735.
33. Sickmeier M., Hamilton J. A., LeGall T., Vacic V., Cortese M. S., Tantos A., et al. (2007). DisProt: The database of disordered proteins. Nucleic Acids Res. 35, 786-793.

34. Mika S., Rost B. (2003). UniqueProt: Creating representative protein sequence sets. Nucleic Acids Res. 31, 3789-3791.
35. Velankar S., McNeil P., Mittard-Runte V., Suarez A., Barrell D., Apweiler R., et al. (2005). E-MSD: An integrated data resource for bioinformatics. Nucleic Acids Res. 33, 211-216.
36. Mészáros B., Simon I., Dosztányi Z. (2009). Prediction of protein binding regions in disordered proteins. PLoS Comput Biol. 5, e1000376.
37. Dosztányi Z., Mészáros B., Simon I. (2009). ANCHOR: web server for predicting protein binding regions in disordered proteins. Bioinformatics. 25, 2745-2746.
38. Müller-Späth S., Soranno A., Hirschfeld V., Hofmann H., Rüegger S., Reymond L., et al. (2010). Charge interactions can dominate the dimensions of intrinsically disordered proteins. Proc. Natl. Acad. Sci. USA. 107, 4451-4457.
39. Soranno A., Koenig I., Borgia M. B., Hofmann H., Zosel F., Nettels D., et al. (2014). Single-molecule spectroscopy reveals polymer effects of disordered proteins in crowded environments. Proc. Natl. Acad. Sci. USA. 111, 4874-4879.
40. Lise S., Jones D. T. (2005). Sequence patterns associated with disordered regions in proteins. Proteins: Struct., Funct., Genet. 58, 144-150.
41. Mao A. H., Crick S. L., Vitalis A., Chicoine C. L., Pappu R. V. (2010). Net charge per residue modulates conformational ensembles of intrinsically disordered proteins. Proc. Natl. Acad. Sci. USA. 107, 8183-8188.
42. Krieger J. M., Fusco G., Lewitzky M., Simister P. C., Marchant J., Camilloni C., et al. (2014). Conformational recognition of an intrinsically disordered protein. Biophys. J. 106, 1771-1779.
43. Iešmantavičius V., Dogan J., Jemth P., Teilum K., Kjaergaard M. (2014). Helical propensity in an intrinsically disordered protein accelerates ligand binding. Angew. Chemie., Int. Ed. Engl. 53, 1548-1551.
44. Huang Y., Liu Z. (2009). Kinetic advantage of intrinsically disordered proteins in coupled folding – binding process : A critical assessment of the " Fly-Casting " mechanism. J. Mol. Biol. 393, 1143-1159.
45. Shammas S. L., Travis A. J., Clarke J. (2013). Remarkably fast coupled folding and binding of the intrinsically disordered transactivation domain of cMyb to CBP KIX. J. Phys. Chem. B. 117, 13346-13356.
46. Rogers J. M., Steward A., Clarke J. (2013). Folding and binding of an intrinsically disordered protein: Fast, but not 'diffusion-limited'. J. Am. Chem. Soc. 135, 1415-1422.
47. Wicky B. I. M., Shammas S. L., Clarke J. (2017). Affinity of IDPs to their targets is modulated by ion-specific changes in kinetics and residual structure. Proc. Natl. Acad. Sci. USA. 114, 9882-9887.
48. Shammas S. L., Travis A. J., Clarke J. (2014). Allostery within a transcription coactivator is predominantly mediated through dissociation rate constants. Proc. Natl. Acad. Sci. U.S.A. 111, 12055-12060.
49. Dahal L., Shammas S. L., Clarke J. (2017). Phosphorylation of the IDP KID modulates affinity for KIX by increasing the lifetime of the complex. Biophys. J. 113, 2706-2712.

50. Crabtree M. D., Borcherds W., Poosapati A., Shammas S. L., Daughdrill G. W., Clarke J. (2017). Conserved helix-flanking prolines modulate IDP:target affinity by altering the lifetime of the bound complex. Biochemistry. 56, 2379-2384.
51. Zhou H. X. (2012). Intrinsic disorder: Signaling via highly specific but short-lived association. Trends Biochem. Sci. 37, 43-48.
52. Borcherds W., Theillet F. X., Katzer A., Finzel A., Mishall K. M., Powell A. T., et al. (2014). Disorder and residual helicity alter p53-Mdm2 binding affinity and signaling in cells. Nat. Chem. Biol. 10, 1000-1002.
53. Ward J. J., Sodhi J. S., McGuffin L. J., Buxton B. F., Jones D. T. (2004). Prediction and functional analysis of native disorder in proteins from the three kingdoms of life. J. Mol. Biol. 337, 635-645.
54. Chen J. W., Romero P., Uversky V. N., Dunker A. K. (2006). Conservation of intrinsic disorder in protein domains and families: II. Functions of conserved disorder. J. Proteome Res. 5, 888-898.
55. van der Lee R., Buljan M., Lang B., Weatheritt R. J., Daughdrill G. W., Dunker A. K., et al. (2014). Classification of intrinsically disordered regions and proteins. Chem. Rev. . 114, 6589-6631.
56. Smits C., Czabotar P. E., Hinds M. G., Day C. L. (2008). Structural plasticity underpins promiscuous binding of the prosurvival protein A1. Structure. 16, 818-829.
57. Czabotar P. E., Lee E. F., van Delft M. F., Day C. L., Smith B. J., Huang D. C. S., et al. (2007). Structural insights into the degradation of Mcl-1 induced by BH3 domains. Proc. Natl. Acad. Sci. USA. 104, 6217-6222.
58. Rogers J. M., Wong C. T., Clarke J. (2014). Coupled folding and binding of the disordered protein PUMA does not require particular residual structure. J. Am. Chem. Soc. 136, 5197-5200.
59. Pace C. N., Grimsley G. R., Scholtz J. M. (2009). Protein ionizable groups: pK values and their contribution to protein stability and solubility. J. Biol. Chem. 284, 13285-13289.
60. Fire E., Gullá S. V., Grant R. A., Keating A. E. (2010). Mcl-1-Bim complexes accommodate surprising point mutations via minor structural changes. Protein Sci. 19, 507-519.
61. Liu Q., Moldoveanu T., Sprules T., Matta-Camacho E., Mansur-Azzam N., Gehring K. (2010). Apoptotic regulation by MCL-1 through heterodimerization. J. Biol. Chem. 285, 19615-19624.
62. Czabotar P. E., Lee E. F., Thompson G. V., Wardak A. Z., Fairlie W. D., Colman P. M. (2011). Mutation to bax beyond the BH3 domain disrupts interactions with pro-survival proteins and promotes apoptosis. J. Biol. Chem. 286, 7123-7131.

A

```
BAK        PLEPNSILGQVGRQLALIGDDINRRYDTEFQNLLE
BAX        QPPQDASTKKLSEALRRIGDELDSNMELQRMIADV
BID        SESQEEIIHNIARHLAQIGDEMDHNIQPTLVRQLA
BIM        EPEDLRPEIRIAQELRRIGDEFNETYTRRVFANDY
BMF        QFLQHRAEVQIARKLQAIADQFHRLHTQQHQQNRD
NOXA_A     NPTRAELPPEFAAQLRKIGDKVYATWSAPDITVVL
NOXA_B     GTRVPADLKDEAAQLRRIGDKVNLRQKLLNLESKL
PUMA       RVEEEEWAREIGAQLRRAADDLNAQYERRRQEEQH
                     .  *    .*..
```

B

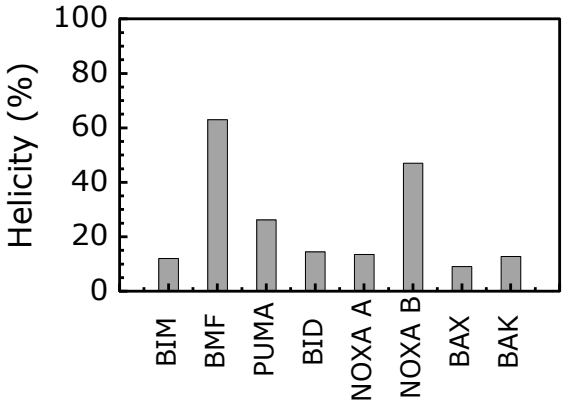

C

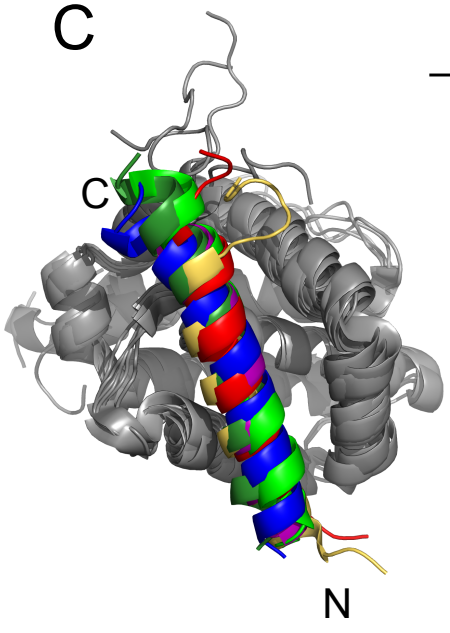

RMSD (Cα)	2ROC	2ROD	2JM6	2PQK	2KBW	3PK1
2ROC		1.942 (172 atoms)	1.927 (152 atoms)	1.490 (165 atoms)	3.143 (176 atoms)	2.421 (161 atoms)
2ROD	1.942 (172 atoms)		1.225 (150 atoms)	1.398 (162 atoms)	3.403 (174 atoms)	1.600 (155 atoms)
2JM6	1.927 (152 atoms)	1.225 (150 atoms)		1.368 (141 atoms)	2.800 (147 atoms)	1.297 (135 atoms)
2PQK	1.490 (165 atoms)	1.398 (162 atoms)	1.368 (141 atoms)		2.360 (164 atoms)	0.662 (157 atoms)
2KBW	3.143 (176 atoms)	3.403 (174 atoms)	2.800 (147 atoms)	2.360 (164 atoms)		2.322 (156 atoms)
3PK1	2.421 (161 atoms)	1.600 (155 atoms)	1.297 (135 atoms)	0.662 (157 atoms)	2.322 (156 atoms)	

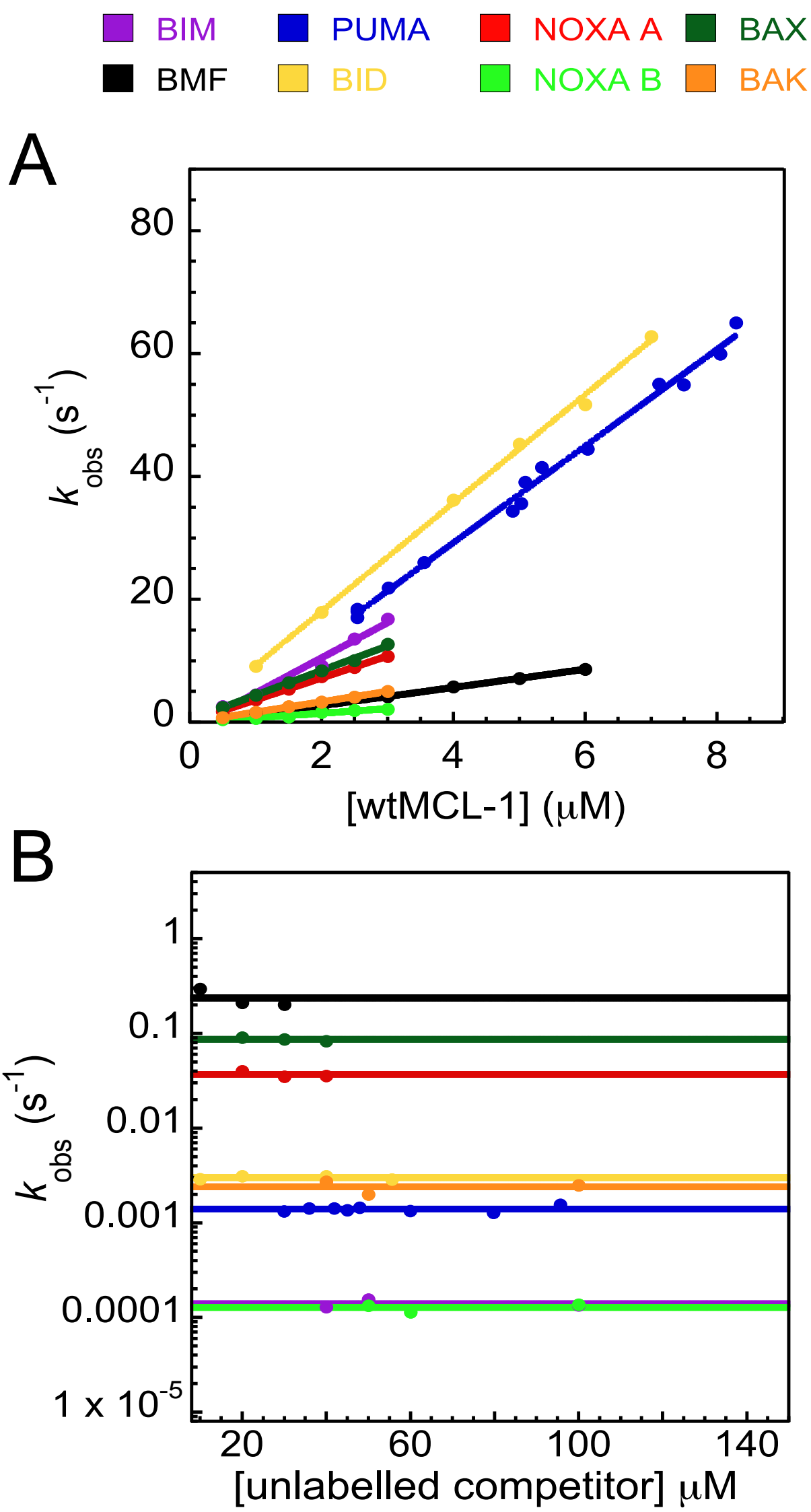
BIM
PUMA
NOXA A
BAX
BMF
BID
NOXA B
BAK
A
80
60
40
20
0
k_{obs} (s^{-1})
0
2
4
6
8
[wtMCL-1] (μM)
B
1
0.1
0.01
0.001
0.0001
1 x 10^{-5}
k_{obs} (s^{-1})
20
60
100
140
[unlabelled competitor] μM

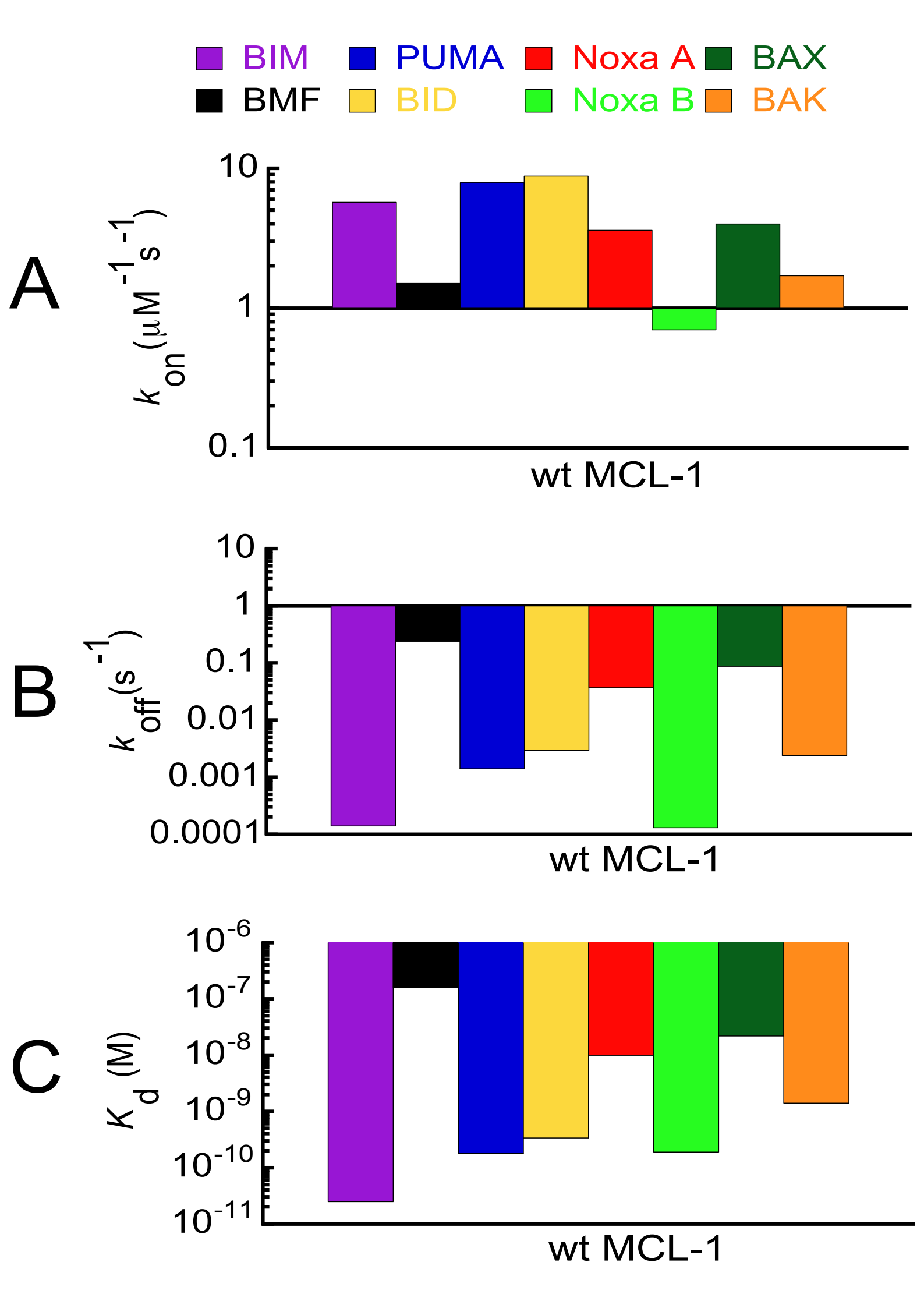
BIM
PUMA
Noxa A
BAX
BMF
BID
Noxa B
BAK
A
10
1
0.1
k_{on} ($\mu M^{-1} s^{-1}$)
wt MCL-1
B
10
1
0.1
0.01
0.001
0.0001
k_{off} (s^{-1})
wt MCL-1
C
10^{-6}
10^{-7}
10^{-8}
10^{-9}
10^{-10}
10^{-11}
K_d (M)
wt MCL-1

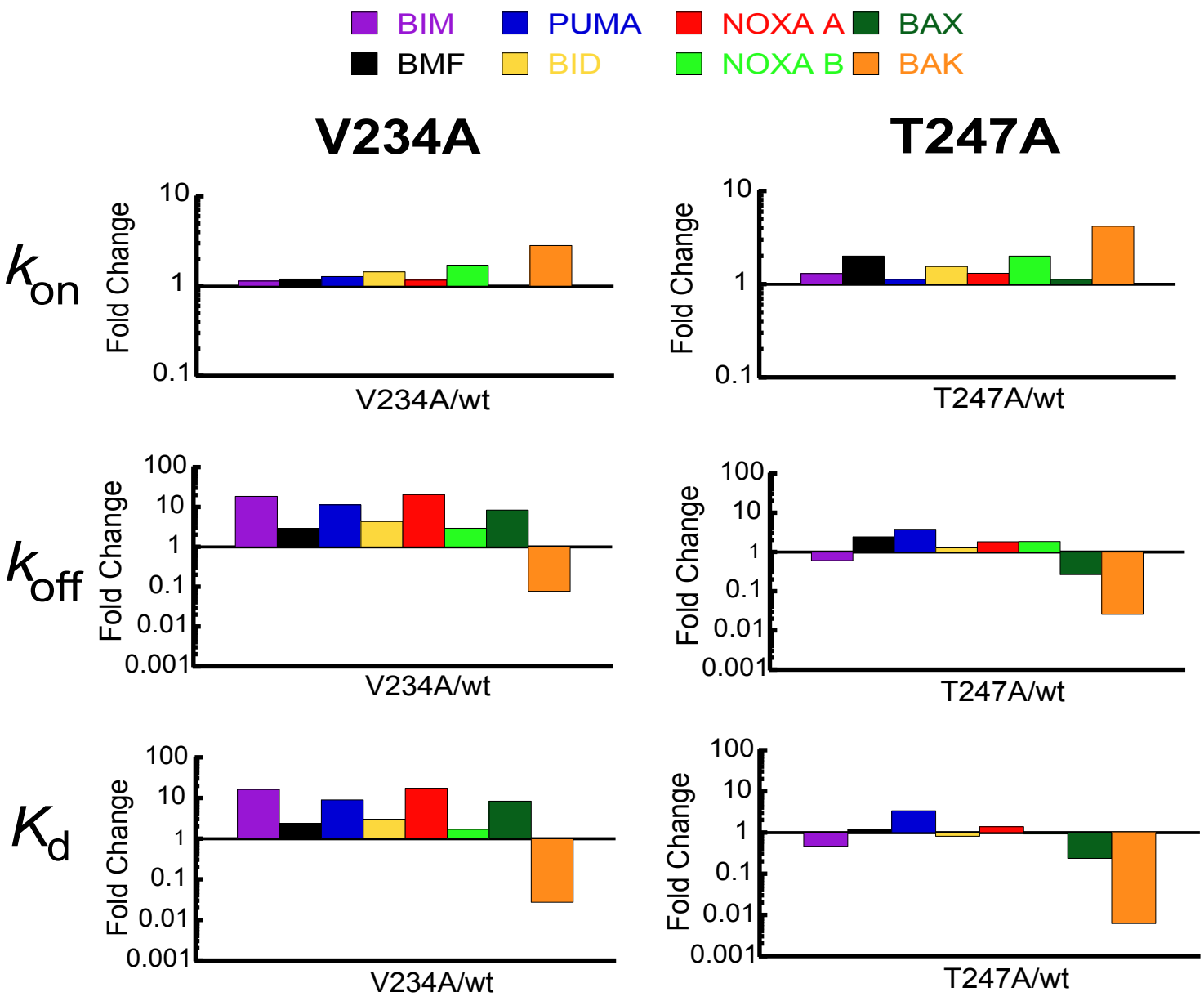
BIM
PUMA
NOXA A
BAX
BMF
BID
NOXA B
BAK
V234A
T247A
k_{on}
k_{off}
K_d
Fold Change
10
1
0.1
100
0.01
0.001
V234A/wt
T247A/wt

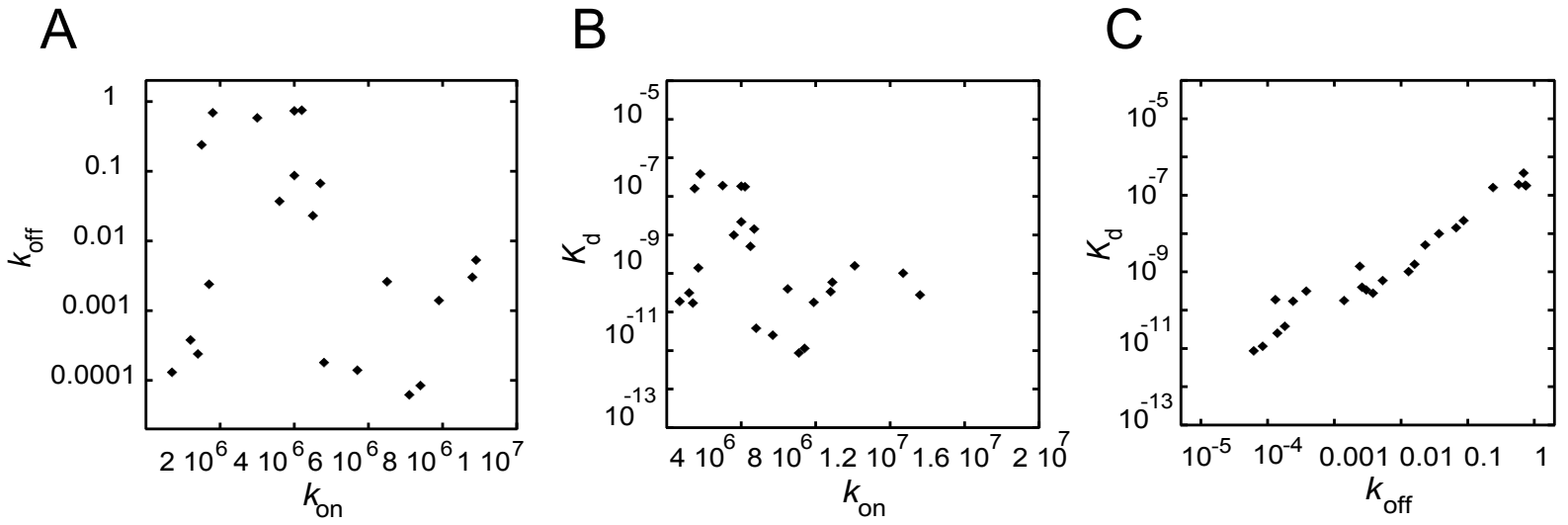
A
B
C
1
0.1
0.01
0.001
0.0001
k_{off}
2 10^6 4 10^6 6 10^6 8 10^6 1 10^7
k_{on}
10^-5
10^-7
10^-9
10^-11
10^-13
K_d
4 10^6 8 10^6 1.2 10^7 1.6 10^7 2 10^7
k_{on}
10^-5
10^-7
10^-9
10^-11
10^-13
K_d
10^-5 10^-4 0.001 0.01 0.1 1
k_{off}

Figure Legends

Fig. 1. BH3 peptides have different sequences and intrinsic helicities but fold to the same structure. (A) Sequence alignments of eight BH3 peptides (PUMA, BID, BIM, BMF, NOXA A, NOXA B, BAK and BAX). For each BH3 peptides the sequences from *Mus musculus* were aligned using Clustal Omega. Absolutely conserved residues are indicated by *, residues where the character of the residue is conserved denoted by a period (.) (B) Percentage residual helicity calculated from mean residual elipticity (MRE) data obtained from Circular Dichorism (CD), see Methods; is shown for the eight N-terminally TAMRA labeled BH3 peptides. The peptides show different degrees of disorder with BAX being least helical and BMF the most helical. (C) Structural alignment of available bound structures of MCL-1 (grey cartoon) with different BH3 peptides (colored cartoon; PUMA - dark blue (Protein Data Bank (PDB) entry: 2ROC[11], *Mus musculus*), NOXA A - red (PDB entry: 2ROD[11], *Mus musculus*), NOXA B - light green (PDB entry: 2JM6[57], *Mus musculus*), BIM – purple (PDB entry: 2PQK[60], *Homo sapiens*), BID- yellow (PDB entry: 2KBW[61], *Homo sapiens*), and BAX- dark green (PDB entry: 3PK1[62], *Homo sapiens*)], built using PyMol. RMSD values calculated from PyMOL for each structural alignment are reported alongside.

Fig. 2. Kinetics data for interactions of BH3 peptides (PUMA, BID, BIM, BMF, NOXA A, NOXA B, BAX and BAK) with wild-type MCL-1. (A) Observed rate constants for BH3 peptides associating with wild-type MCL-1 under pseudo-first-order conditions with MCL-1 in excess. (B) Observed rate constants for dissociation of BH3 peptides from wild-type MCL-1 obtained by mixing with an excess of out-competing peptide. Colors of the data points represent each BH3 peptides as shown in the legend at the top of the Figure.

Data for kinetics of PUMA interacting with MCL-1 was obtained from Rogers et al. 2014[18]. Note: unlike other BH3 peptides investigated in this study PUMA is not labeled with TAMRA or any other extrinsic dye[18].

Fig. 3. Representation of kinetic and thermodynamic parameters**.** (A) Association rate constant (k_{on}) (B) Dissociation rate constant (k_{off}) and (C) Equilibrium dissociation constant (K_d) for BH3 peptides binding to wt MCL-1. Larger differences in k_{off} than k_{on} are observed (note differences in scale of y-axes). The differences in K_d reflect the difference in k_{off}. Colors for BH3 peptides as shown at the top of the figure. Data for PUMA are taken from Rogers et al. [18].

Fig. 4. Fold-change in thermodynamics and kinetic parameters for BH3 peptides binding to MCL-1 mutants (V234A, left column and T247A, right column). Top: Fold-change in association kinetics (k_{on}). Although most BH3 peptides bind slightly faster to mutant MCL-1, changes in k_{on} upon mutation of MCL-1 are <5-fold for all the BH3 peptides investigated. Middle: Fold-change in association kinetics (k_{off}) (Note different scale compared to top row). Change in k_{off} upon mutation of MCL-1 for all the BH3 peptides investigated are more significant and very different, with a maximum change of 40-fold. Bottom: Fold-change in Equilibrium constant (K_d). Changes in (K_d) upon mutation of MCL-1 for all the BH3 peptides investigated reflect changes in k_{off} with maximum changes of ~40-fold. The color for BH3 peptides as shown at the top of the figure. Data for PUMA are taken from Rogers et al. [18].

Fig. 5. Correlation between kinetic and thermodynamic parameters studied for all BH3 peptides interacting with wild-type and mutants of MCL-1. A.) k_{off} vs k_{on}; no co-relation is observed between association (k_{on}) and dissociation kinetics (k_{off}). B) K_d vs k_{on}; no co-

relation is observed between equilibrium constant (K_d) and association kinetics (k_{on}). C) K_d vs k_{off}; a clear co-relation is observed between equilibrium constant (K_d) and dissociation kinetics (k_{off}). Note that the plots shown are in log scale.

Tables

Table 1. Kinetic and thermodynamic parameters of wild-type MCL-1 interacting with different BH3 peptides

Protein	BH3 peptides	k_{on} ($M^{-1}s^{-1}$) (x 10^6)	k_{off} (s^{-1}) (x 10^{-3})	K_d (M) (x 10^{-9})
wt MCL-1	PUMA	7.9 ± 0.2	1.4 ± 0.03	0.18 ± 0.01
	BID	8.8 ± 0.2	3.0 ± 0.1	0.34 ± 0.01
	NOXA A	3.6 ± 0.1	37 ± 2	10 ± 0.5
	NOXA B	0.7 ± 0.1	0.13 ± 0.01	0.19 ± 0.03
	BMF	1.5 ± 0.1	240 ± 30	160 ± 20
	BIM	5.7 ± 0.4	0.14 ± 0.01	0.025 ± 0.002
	BAX	4.0 ± 0.1	87 ± 2	22 ± 0.8
	BAK	1.7 ± 0.03	2.4 ± 0.2	1.4 ± 0.1

K_d is calculated from kinetic rate constants ($K_d = k_{off} / k_{on}$). Errors reported in k_{on} and k_{off} are errors from the linear fit of observed rate constants.
Errors for K_d were propagated using standard equations. Data for PUMA was obtained from Rogers et al. 2014[18]

Table 2. Kinetic and thermodynamic parameters of mutant forms of MCL-1 interacting with different BH3 peptides

Protein	BH3 peptides	k_{on} ($M^{-1}s^{-1}$) (x 10^6)	k_{off} (s^{-1}) (x 10^{-3})	K_d (M) (x 10^{-9})	$\Delta\Delta G$ (kcal.mol^{-1})
V234A MCL-1	PUMA	10.1 ± 0.05	16 ± 0.04	1.6 ± 0.01	1.3 ± 0.03
	BID	12.7 ± 0.6	13 ± 0.4	1.0 ± 0.06	0.64 ± 0.04
	NOXA A	4.2 ± 0.04	750 ± 30	179 ± 7	1.7 ± 0.04
	NOXA B	1.2 ± 0.04	0.37 ± 0.01	0.32 ± 0.02	0.31 ± 0.1
	BMF	1.8 ± 0.04	690 ± 10	383 ± 9	0.52 ± 0.08
	BIM	6.5 ± 0.3	2.6 ± 0.1	0.40 ± 0.02	1.6 ± 0.06
	BAX	4.0 ± 0.3	730 ± 60	183 ± 21	1.3 ± 0.07
	BAK	4.8 ± 0.1	0.18 ± 0.02	0.038 ± 0.004	-2.1 ± 0.08
MCL-1 T247A	PUMA	8.9 ± 0.6	5.3 ± 0.3	0.60 ± 0.05	0.71 ± 0.06
	BID	13.6 ± 0.3	3.8 ± 0.4	0.28 ± 0.03	-0.11 ± 0.07
	NOXA A	4.7 ± 0.1	67 ± 2	14.3 ± 0.5	0.21 ± 0.04
	NOXA B	1.4 ± 0.01	0.24 ± 0.01	0.17 ± 0.01	-0.07 ± 0.10
	BMF	3.0 ± 0.03	580 ± 70	193 ± 21	0.11 ± 0.10
	BIM	7.4 ± 0.5	0.084 ± 0.001	0.011 ± 0.0008	-0.49 ± 0.06
	BAX	4.5 ± 0.3	23 ± 1	5.1 ± 0.4	-0.87 ± 0.05
	BAK	7.1 ± 0.2	0.062 ± 0.001	0.008 ± 0.0002	-3.06 ± 0.04

K_d is calculated from kinetic rate constants ($K_d = k_{off} / k_{on}$) and $\Delta\Delta G = RT \ln (K_{d\ mutant} / K_{d\ wt})$. Errors reported in k_{on} and k_{off} are errors from the linear fit of observed rate constants.
Errors for K_d, $\Delta\Delta G$ were propagated using standard equations. Data for PUMA was obtained from Rogers et al. 2014[18].

Supporting Information

Promiscuous and selective: how intrinsically disordered BH3 proteins interact with their pro-survival partner MCL-1.

Liza Dahal, Tristan O.C. Kwan, Jeffery J. Hollins and Jane Clarke[1]

[1]Corresponding author, Email: jc162@cam.ac.uk

Department of Chemistry, University of Cambridge, Lensfield Road, Cambridge, CB2 1EW

Supplementary Figures

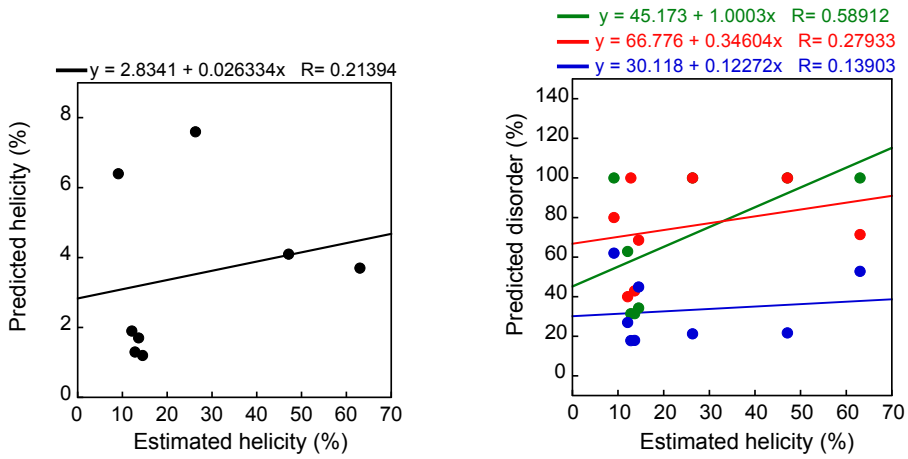

Fig. S1. No correlation was observed between estimated helicity (%) calculated from CD experiments and predicted helicity (%) or predicted disorder (%) calculated from online tools. Left: Estimated helicity (%) calculated from CD[1] vs predicted helicity (%) using Agadir[2-4] (black). Right: Estimated helicity (%) calculated from CD[1] vs predicted disorder (%) using online tools PONDR VSL2[5-12] (green), ESpritz (X-Ray)[13-17] (red), and ANCHOR[18, 19] (blue).

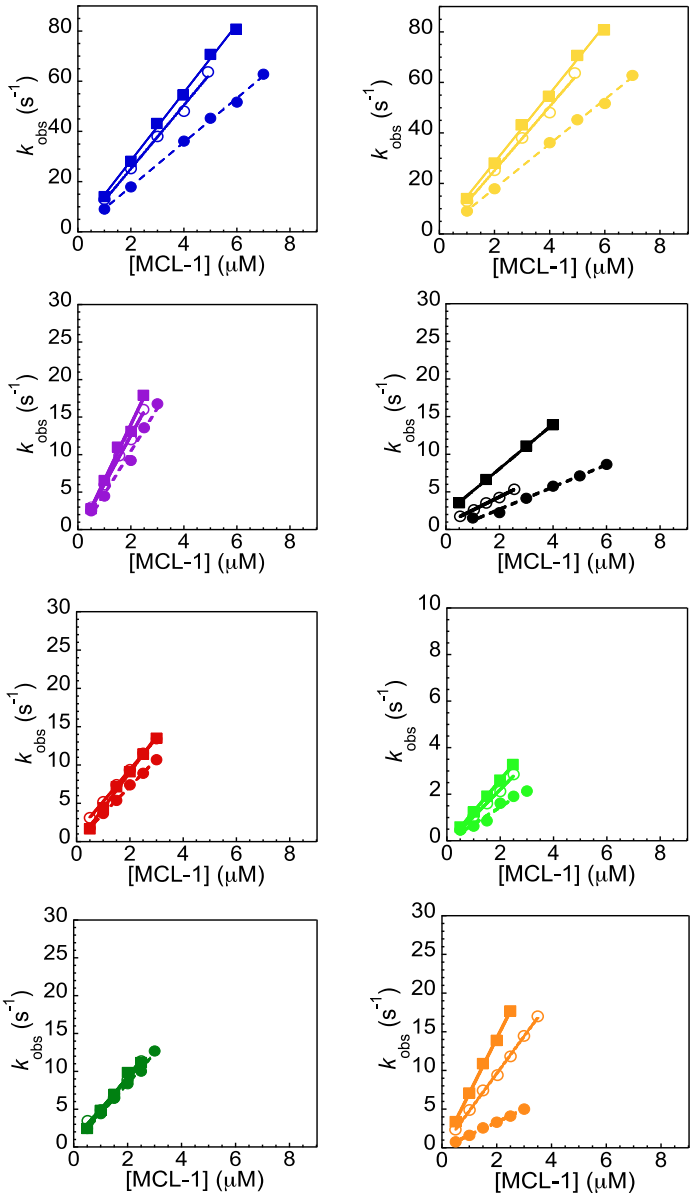

Fig. S2. Comparing association kinetics data for all BH3 peptides (PUMA – dark blue, BID – yellow, BIM – purple, BMF – black, NOXA A – red, NOXA B – light green, BAX – dark green and BAK – orange) interacting with wt and mutants of MCL-1. Observed rate constants for BH3 peptides associating with MCL-1 under pseudo-first-order conditions with MCL-1 in excess. Closed circles with dotted line fit represent data obtained for wild-type MCL-1. Open circles represent data obtained for V234A MCL-1 and closed squares represent data for T247A MCL-1. Compared to wt, faster association kinetics is observed for all BH3 peptides interacting with mutants of MCL-1 except for BAX. Data for kinetics of PUMA interacting with MCL-1 was obtained from Rogers et al. 2014[20].

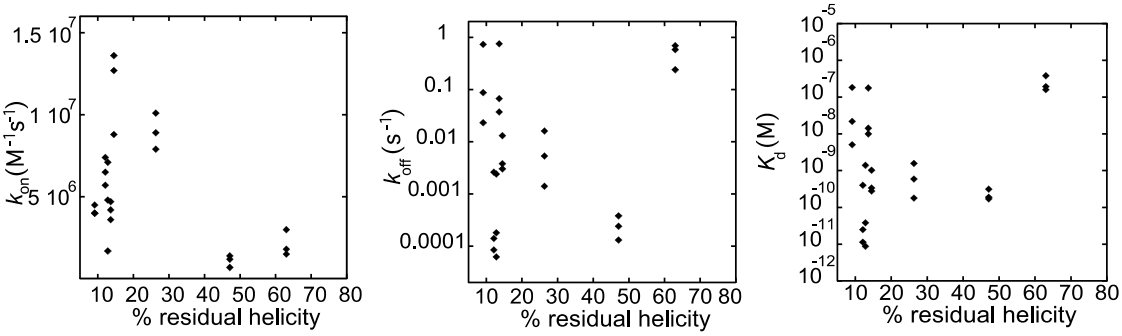

Fig. S3. No correlation observed between percentage (%) residual helicity and kinetic and thermodynamic parameters studied for all BH3 peptides interacting with wild-type and mutants of MCL-1. Left: k_{on} vs % residual helicity; Centre: k_{off} vs % residual helicity; Right: K_d vs % residual helicity.

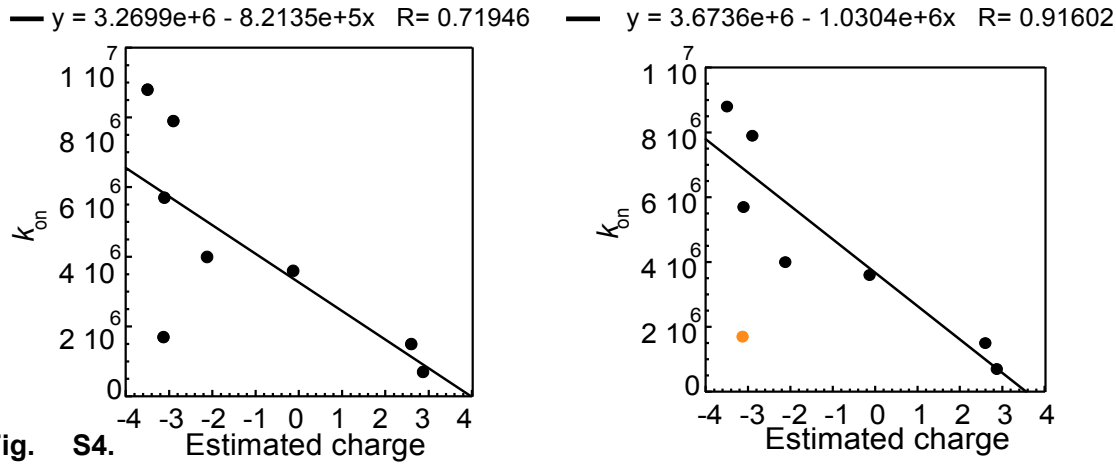

Fig. S4. Rate constants for association between wt MCL-1 and BH3 peptides correlate with peptide charge. Left: k_{on} vs estimated charge, the straight line fit includes data for all BH3 peptides; Right : k_{on} vs estimated charge, the straight line fit includes data points for all BH3 peptides except BAK (shown in orange) which seems to be an outlier. The charge on each peptide was calculated using pK_a values reported for each amino acid for model peptides and corrected for the addition of TAMRA dye at the N-terminus[21].

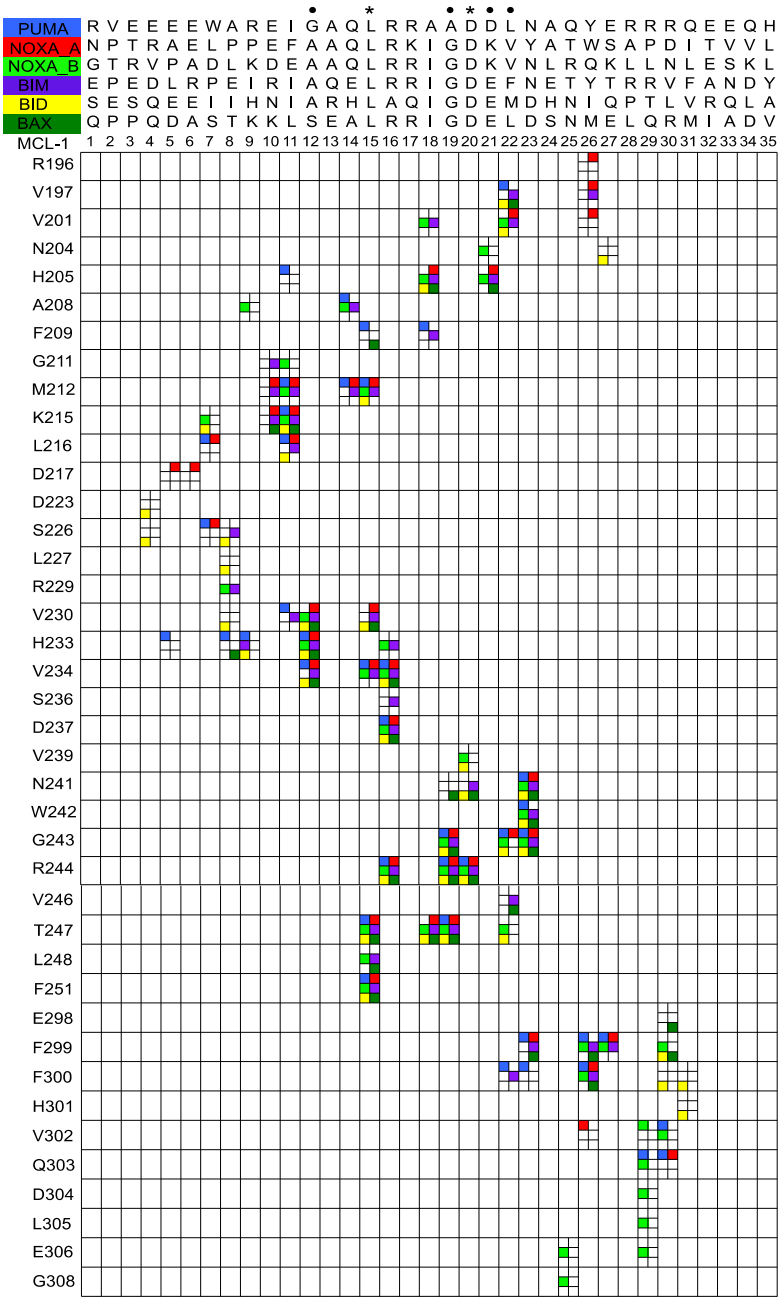

Fig. S5. Contact map for interactions between six BH3 peptides and MCL1. The contacts with MCL-1 for PUMA (blue) was obtained using PDB structure 2ROC[22], for NOXA A (red) 2ROD[22], for NOXA B (light green) 2JM6[23], for BIM (purple) 2PQK[24], for BID (yellow) 2KBW[25] and for BAX (dark green) 3PK1[26].Contacts between BH3 peptide and MCL-1 was defined between any non-hydrogen atom within 4Å distance. Note that three of these are for Murine peptides and proteins (2ROC, 2ROD, 2JM6) and three for human complexes (2PQK, 2KBW, 3PK1).

References

1. Muñoz V., Serrano L. (1995). Elucidating the folding problem of helical peptides using empirical parameters. II. Helix macrodipole effects and rational modification of the helical content of natural peptides. J. Mol. Biol. 245, 275-296.
2. Munoz V., Serrano L. (1994). Elucidating the folding problem of helical peptides using empirical parameters. Nat. Struct. Biol. 1, 399-409.
3. Munoz V., Serrano L. (1997). Development of the multiple sequence approximation within the AGADIR model of a-Helix formation: Comparison with Zimm–Bragg and Lifson–Roig Formalisms. Biopolymers. 41, 495-509.
4. Lacroix E., Viguera A. R., Serrano L. (1998). Elucidating the folding problem of alpha-helices: local motifs, long- range electrostatics, ionic-strength dependence and prediction of NMR parameters. J. Mol. Biol. 284, 173-191.
5. Garner E., Romero P., Dunker A. K., Brown C. J., Obradovic Z. (1999). Predicting binding regions within disordered proteins. Genome Inf. Ser. 10, 41-50.
6. Li X., Romero P., Rani M., Dunker A. K., Obradovic Z. (1999). Prediction protein disorder for N-, C-, and internal regions. Genome Inf. Ser. 10, 30-40.
7. Romero P., Obradovic Z., Dunker A. K. (1997). Sequence data analysis for long disordered regions prediction in the calcineurin family. Genome Inf. Ser. 8, 110-124.
8. Uversky V. N., Gillespie J. R., Fink A. L. (2000). Why are 'natively unfolded' proteins unstructured under physiologic conditions? Proteins: Struct., Funct., Genet. 41, 415-427.
9. Romero P., Obradovic Z., Li X., Garner E. C., Brown C. J., Dunker A. K. (2001). Sequence complexity of disordered protein. Proteins: Struct., Funct., Genet. 42, 38-48.
10. Vucetic S., Brown C. J., Dunker A. K., Obradovic Z. (2003). Flavors of protein disorder. Proteins: Struct., Funct., Genet. 52, 573-584.
11. Radivojac P., Obradović Z., Brown C. J., Dunker A. K. (2003). Prediction of boundaries between intrinsically ordered and disordered protein regions. Pac. Symp. Biocomput. 227, 216-227.
12. Obradovic Z., Peng K., Vucetic S., Radivojac P., Brown C. J., Dunker A. K. (2003). Predicting intrinsic disorder from amino acid sequence. Proteins: Struct., Funct., Genet. 53, 566-572.
13. Pollastri G., Przybylski D., Rost B., Baldi P. (2002). Improving the prediction of protein secondary structure in three and eight classes using recurrent neural networks and profiles. Proteins: Struct., Funct., Genet. 47, 228-235.
14. Sperduti A., Starita A. (1997). Supervised neural networks for the classification of structures. Neural Networks, IEEE Transactions on 8, 714-735.
15. Sickmeier M., Hamilton J. A., LeGall T., Vacic V., Cortese M. S., Tantos A., et al. (2007). DisProt: The database of disordered proteins. Nucleic Acids Res. 35, 786-793.
16. Mika S., Rost B. (2003). UniqueProt: Creating representative protein sequence sets. Nucleic Acids Res. 31, 3789-3791.

17. Velankar S., McNeil P., Mittard-Runte V., Suarez A., Barrell D., Apweiler R., et al. (2005). E-MSD: An integrated data resource for bioinformatics. Nucleic Acids Res. 33, 211-216.
18. Mészáros B., Simon I., Dosztányi Z. (2009). Prediction of protein binding regions in disordered proteins. PLoS Comput Biol. 5, e1000376.
19. Dosztányi Z., Mészáros B., Simon I. (2009). ANCHOR: web server for predicting protein binding regions in disordered proteins. Bioinformatics. 25, 2745-2746.
20. Rogers J. M., Oleinikovas V., Shammas S. L., Wong C. T., De Sancho D., Baker C. M., et al. (2014). Interplay between partner and ligand facilitates the folding and binding of an intrinsically disordered protein. Proc. Natl. Acad. Sci. U.S.A. 111, 15420-15425.
21. Pace C. N., Grimsley G. R., Scholtz J. M. (2009). Protein ionizable groups: pK values and their contribution to protein stability and solubility. J. Biol. Chem. 284, 13285-13289.
22. Day C. L., Smits C., Fan F. C., Lee E. F., Fairlie W. D., Hinds M. G. (2008). Structure of the BH3 domains from the p53-inducible BH3-only proteins Noxa and Puma in complex with Mcl-1. J. Mol. Biol. 380, 958-971.
23. Czabotar P. E., Lee E. F., van Delft M. F., Day C. L., Smith B. J., Huang D. C. S., et al. (2007). Structural insights into the degradation of Mcl-1 induced by BH3 domains. Proc. Natl. Acad. Sci. USA. 104, 6217-6222.
24. Fire E., Gullá S. V., Grant R. A., Keating A. E. (2010). Mcl-1-Bim complexes accommodate surprising point mutations via minor structural changes. Protein Sci. 19, 507-519.
25. Liu Q., Moldoveanu T., Sprules T., Matta-Camacho E., Mansur-Azzam N., Gehring K. (2010). Apoptotic regulation by MCL-1 through heterodimerization. J. Biol. Chem. 285, 19615-19624.
26. Czabotar P. E., Lee E. F., Thompson G. V., Wardak A. Z., Fairlie W. D., Colman P. M. (2011). Mutation to bax beyond the BH3 domain disrupts interactions with pro-survival proteins and promotes apoptosis. J. Biol. Chem. 286, 7123-7131.